

1 **Prognostic Insights from Longitudinal Multicompartment Study of Host-Microbiota Interactions in**  
2 **Critically Ill Patients.**

3  
4 Georgios D. Kitsios, MD, PhD<sup>1,2\*</sup>; Khaled Sayed, PhD<sup>3,4</sup>; Adam Fitch, MS<sup>2</sup>; Haopu Yang MDc<sup>5</sup>; Noel Britton,  
5 PhD<sup>6</sup>; Faraaz Shah, MD, MPH<sup>1,7</sup>; William Bain, MD<sup>1,7</sup>; John W. Evankovich, MD;<sup>1</sup> Shulin Qin, MD, PhD<sup>1,2</sup>;  
6 Xiaohong Wang, MS<sup>1,2</sup>; Kelvin Li, MS<sup>2</sup>; Asha Patel, BS<sup>1,2</sup>; Yingze Zhang, PhD<sup>1</sup>; Josiah Radder, MD, PhD<sup>1,2</sup>,  
7 Charles Dela Cruz, MD, PhD<sup>1</sup>; Daniel A Okin, MD PhD<sup>8</sup>; Ching-Ying Huang, MS<sup>8</sup>; Daria van Tyne, PhD<sup>9</sup>;  
8 Panayiotis V. Benos, PhD<sup>3</sup>; Barbara Methé, PhD<sup>1,2</sup>; Peggy Lai, MD<sup>8</sup>; Alison Morris, MD, MS<sup>1,2^</sup>; Bryan J.  
9 McVerry, MD<sup>1,2^</sup>

10  
11 \*Corresponding author

12 ^Co-senior authors

13  
14 **Institutions/affiliations:**

15 1 - Division of Pulmonary, Allergy, Critical Care and Sleep Medicine, University of Pittsburgh, Pittsburgh, PA,  
16 USA

17 2 - Center for Medicine and the Microbiome, University of Pittsburgh, Pittsburgh, PA, USA

18 3 - Department of Epidemiology, University of Florida, Gainesville, FL, USA.

19 4 - Department of Electrical and Computer Engineering & Computer Science, University of New Haven, West  
20 Haven, CT, USA

21 5- School of Medicine, Tsinghua University, Beijing, China

22 6- Division of Pulmonary Critical Care Medicine, Department of Medicine, Johns Hopkins University School of  
23 Medicine, Baltimore, Maryland, USA

24 7- Veteran's Affairs Pittsburgh Healthcare System, Pittsburgh, PA, USA.

25 8- Division of Pulmonary and Critical Care Medicine, Massachusetts General Hospital and Harvard Medical  
26 School, Boston, MA, USA

27 9- Division of Infectious Diseases, Department of Medicine, University of Pittsburgh, Pittsburgh, PA, USA

28

29

30 Corresponding author:

31 Georgios D. Kitsios, MD, PhD

32 Assistant Professor of Medicine

33 Division of Pulmonary, Allergy, Critical Care and Sleep Medicine

34 University of Pittsburgh Medical Center

35 Address: UPMC Montefiore Hospital, NW628, 3459 Fifth Avenue, Pittsburgh, PA 15213

36 Email: [kitsiosg@upmc.edu](mailto:kitsiosg@upmc.edu)

37

38

39 **Author's contributions:**

40 **Author A:** Conceptualization, Methodology, Validation, Investigation, Resources, Writing - Original Draft,  
41 Writing - Review & Editing, Visualization, Project administration; **Georgios D. Kitsios:** Conceptualization,  
42 Methodology, Validation, Formal analysis, Investigation, Resources, Writing - Original Draft, Writing - Review &  
43 Editing, Visualization, Supervision, Project administration, Funding acquisition; **Authors B, C, D:** Investigation,  
44 Writing - Review & Editing

45

46 **Conflicts of Interest:** Dr. Kitsios has received research funding from Karius, Inc and Pfizer, Inc, both  
47 unrelated to this project. Dr. Morris has received research funding from Pfizer, Inc, unrelated to this project. Dr  
48 McVerry has received consulting fees from Boehringer Ingelheim, BioAegis, and Synairgen Research, Ltd.  
49 unrelated to this work. All other authors disclosed no conflict of interest.

50 **Funding information:** Dr. Kitsios: University of Pittsburgh Clinical and Translational Science Institute, COVID-  
51 19 Pilot Award; NIH (R03 HL162655); Dr. Benos: NIH (R01 HL157879; R01 HL127349, R01DK130294); Dr.  
52 McVerry: NIH (P01 HL114453); Dr. Bain: Veterans Affairs (IK2BX004886); Dr. Lai: Massachusetts General  
53 Hospital Translational and Clinical Research Center, supported by Grant 1UL1TR002541

54

55

56 **Abstract**

57 Critical illness can disrupt the composition and function of the microbiome, yet comprehensive longitudinal  
58 studies are lacking. We conducted a longitudinal analysis of oral, lung, and gut microbiota in a large cohort of  
59 479 mechanically ventilated patients with acute respiratory failure. Progressive dysbiosis emerged in all three  
60 body compartments, characterized by reduced alpha diversity, depletion of obligate anaerobe bacteria, and  
61 pathogen enrichment. Clinical variables, including chronic obstructive pulmonary disease, immunosuppression,  
62 and antibiotic exposure, shaped dysbiosis. Notably, of the three body compartments, unsupervised clusters of  
63 lung microbiota diversity and composition independently predicted survival, transcending clinical predictors,  
64 organ dysfunction severity, and host-response sub-phenotypes. These independent associations of lung  
65 microbiota may serve as valuable biomarkers for prognostication and treatment decisions in critically ill  
66 patients. Insights into the dynamics of the microbiome during critical illness highlight the potential for  
67 microbiota-targeted interventions in precision medicine.

68

69

70

71 **Keywords:** microbiome, critical illness, dysbiosis, precision medicine, biomarkers

72 .

## 73 Introduction

74 Microbiota play a critical role in maintaining homeostasis and overall health. However, during critical  
75 illness, such as acute respiratory failure (ARF), microbial communities can be severely disrupted.<sup>1,2</sup> Such  
76 disruptions, characterized by deviations from a healthy microbial composition and diversity, may occur early in  
77 the hospital stay and have been associated with worse clinical outcomes.<sup>3-5</sup> Previous research has primarily  
78 focused on cross-sectional analyses of microbiota within individual body sites, neglecting potential interactions  
79 between different compartments and the longitudinal evolution of microbial communities. Moreover, the  
80 influence of patient-level factors and therapeutic interventions, including antimicrobial therapies, on the  
81 microbiome of critically ill patients remains poorly understood, partly due to limitations of scale in studies  
82 published to date.

83 Precision medicine approaches in ARF have predominantly focused on host factors.<sup>6</sup> For instance,  
84 identifying distinct subphenotypes based on patterns of host response biomarkers measured in plasma  
85 samples (hyper- vs. hypo-inflammatory) has demonstrated prognostic value.<sup>7-9</sup> Hyperinflammatory patients  
86 exhibit elevated levels of injury and inflammation biomarkers, more severe organ dysfunction, worse prognosis,  
87 and may have distinct responses to treatments.<sup>8</sup> However, the role of respiratory or intestinal microbiota in  
88 modulating host responses and their contributions to defined subphenotypes are still not well understood.  
89 Furthermore, limited data are available regarding the potential influence of respiratory microbiota on systemic  
90 host responses measured in plasma or localized inflammation within the lungs.<sup>10</sup> To advance precision  
91 medicine approaches that take into account the microbial side of the critically ill host, it is crucial to understand  
92 the dynamics of the microbiome and its relationship with host biological factors, clinical diagnoses, and  
93 therapeutic interventions in critical illness.

94 To address these knowledge gaps, we conducted a longitudinal assessment of the microbiome in a  
95 large cohort of 479 ARF patients, specifically focusing on three key body sites: the oral cavity, lungs, and gut.  
96 By integrating bacterial and fungal community profiles with host response biomarkers measured in plasma and  
97 lower respiratory tract (LRT) samples, we examined the temporal associations between patient-level factors  
98 and therapeutic interventions on microbial communities. We derived unsupervised clusters of microbiota and

99 determined their associations with host-response subphenotypes and clinical outcomes. Finally, we validated  
100 our findings in two separate cohorts with a total of 146 patients with COVID-19-associated ARF.

## 101 **Results**

### 102 Cohort Description:

103 We performed discovery analyses in a cohort of 479 patients with ARF who received invasive  
104 mechanical ventilation (IMV) via endotracheal intubation in UPMC Intensive Care Units (ICUs) (**UPMC-ARF**  
105 **cohort**), and then independent validation analyses in two cohorts of critically ill patients with COVID-19  
106 pneumonia (49 patients at UPMC [**UPMC-COVID cohort**], and 97 patients at Massachusetts General Hospital  
107 ICUs, **MGH-COVID cohort**).

108 In the UPMC-ARF cohort, we enrolled patients with non-COVID etiologies of ARF between March 2015  
109 and June 2022. We collected baseline research biospecimens within 72hrs from intubation, including blood for  
110 separation of plasma, oropharyngeal swabs (oral samples), endotracheal aspirates (ETA) collected for  
111 research or excess bronchoalveolar lavage fluid (BALF) from clinical bronchoscopy (lung samples), and rectal  
112 swabs or stool (gut samples).<sup>3,11,12</sup> We repeated research biospecimen sampling between days 3-6 (middle  
113 interval) and days 7-12 (late interval) post-enrollment for subjects who remained in the ICU. We extracted DNA  
114 and performed next-generation sequencing (bacterial 16S rRNA gene sequencing [16S-Seq] for all available  
115 samples; fungal Internal Transcribed Spacer sequencing [ITS-Seq] targeting the regions 1 and 2 of the ITS  
116 rRNA gene, and Nanopore DNA metagenomics for a subset of samples) to profile microbiota in the oral, lung  
117 and gut communities, respectively.<sup>3,12,13</sup> We measured biomarker proteins in plasma samples and ETA/BALF  
118 supernatants with Luminex panels to profile systemic and regional (lung) host responses.<sup>7,10</sup>

119 Patients had a median (interquartile range) age of 59.6 (46.7-68.7) years, 54.4% were men and 90.2%  
120 were whites (Table 1). At the time of enrollment, 25.0% of patients were diagnosed with Acute Respiratory  
121 Distress Syndrome (ARDS per the Berlin definition<sup>14</sup>) and 39.8% with pneumonia, 86.8% were receiving  
122 systemic antibiotics, and 64.8% received corticosteroids for various indications. By 60 days, 26.9% of patients  
123 had died. Among the 350 patients who survived hospitalization, 48.8% were discharged to their home, with the  
124 remainder requiring additional longer-term care.

125 In the UPMC-COVID cohort, from April 2020 through February 2022 we enrolled 49 patients with  
126 COVID-19 ARDS requiring IMV and obtained longitudinal plasma and ETA samples at baseline, middle and  
127 late intervals (Table S1). We performed 16S sequencing for bacteria and measured host response biomarkers  
128 in both sample types. In the MGH-COVID cohort, from April 2020 to May 2021 we enrolled 97 hospitalized  
129 patients, obtained serial lung (sputum or ETA) and stool (gut) samples (Table S1) and performed Illumina  
130 metagenomics.<sup>15</sup> To contextualize microbiota analyses from critically ill patients, we incorporated previously  
131 generated 16S-Seq data from upper respiratory tract (URT), LRT and stool samples collected from healthy  
132 volunteers (**Healthy Controls**), as previously described in smaller cross-sectional studies from our group.<sup>11,12</sup>

### 134 Progressive dysbiosis of microbial communities in three body compartments.

135 Among all three cohorts and healthy controls, we analyzed a total of 2557 clinical samples and 233  
136 experimental control samples, with the latter obtained either during patient sampling at the bedside or during  
137 sample processing in the laboratory. In an initial quality control step, we demonstrated robust detection of  
138 bacterial 16S reads in oral, lung and gut samples in the UPMC-ARF cohort compared to negative controls  
139 (Figure S1A-B). We also found that rectal swabs not coated by stool (“unsoiled” swabs) had systematic  
140 differences in bacterial load (16S rRNA gene copies by qPCR) and beta diversity (Manhattan distances)  
141 compared to stool or visibly “soiled” rectal swabs (Figure S1C-D). Therefore, we excluded “unsoiled” rectal  
142 swabs from further analyses because they may not offer sufficient representation of gut microbiota.<sup>11</sup>

143 Samples from critically ill patients had significantly lower alpha diversity (Shannon index) in each  
144 compartment compared to corresponding healthy control samples. Alpha diversity further declined in all three  
145 body compartments across longitudinal samples (Figure 1A). Similarly, baseline ICU samples had markedly  
146 significant differences in beta diversity from healthy controls (Figure 1B). Taxonomic composition comparisons  
147 showed depletion of multiple commensal taxa in ICU samples, with significant enrichment for *Staphylococcus*  
148 in oral and lung samples, and *Anaerococcus* and *Staphylococcus* in gut samples (Figure 1C-D-E). Among ICU  
149 samples, bacterial load quantification by 16S qPCR confirmed that the LRT had significantly lower biomass  
150 compared to URT (oral) and gastrointestinal tract (Figure 1F).

151 We then examined the compositional similarity (Bray-Curtis indices) between compartments to  
152 understand the relationship between the low biomass (lung) vs. high biomass (oral and gut) communities. We  
153 found higher similarity between oral-lung vs. gut-lung communities in the baseline and middle intervals (Figure  
154 1G). Taxonomic comparisons between compartments revealed that no specific taxa were systematically  
155 different between oral and lung microbiota (Figure 1H), whereas in gut-lung comparisons, lung communities  
156 were enriched for typical respiratory commensals (e.g. *Rothia*, *Veillonella*, *Streptococcus*) and gut communities  
157 for gut commensals (e.g. *Bacteroides*, *Lachnoclostridium*, *Lachnospiraceae\_uncl*) (Figure 1I). We specifically  
158 tested whether certain patients had enrichment for gut-origin bacteria in their oral or lung samples despite no  
159 overall enrichment of the lung compartment for gut bacteria. We found that 4.8% and 8.1% of oral and lung  
160 samples, respectively, had >30% relative abundance for gut-origin bacteria (Fisher's test  $p=0.03$ , Figure S2A),  
161 with progressively increased enrichment over time (Fisher's test = 0.02, Figure S2B) in lung samples.  
162 Importantly, the gut-origin taxa enrichment in these lung samples could not be fully explained by oropharyngeal  
163 colonization with such taxa (Figure S2C). Taken together, these multi-site analyses point to the oral cavity as  
164 the primary source of lung microbiota, which could be seeded by micro-aspiration along the respiratory tract's  
165 gravitational gradient. At the same time, our analyses also provided evidence for gut-origin bacteria enrichment  
166 in the LRT in a subset of critically ill patients.

167 We next examined the longitudinal composition of microbial communities by classifying bacteria in  
168 terms of their oxygen requirements (obligate anaerobes, facultative anaerobes, aerobes, microaerophiles,  
169 variable or unclassifiable) and plausible respiratory pathogenicity (oral commensals, recognized respiratory  
170 pathogens or other).<sup>12</sup> In both oral and lung communities, we found a progressive decline in the relative  
171 abundance of obligate anaerobes over time. There was, however, no corresponding change in the gut  
172 composition of anaerobic (obligate or facultative) bacteria over time (Figure 2A-B). Stratified by plausible  
173 pathogenicity, we found a progressive decline of oral commensal bacteria in all three compartments, with a  
174 corresponding increase in pathogen abundance (Figure 2C-D). Fungal ITS sequencing showed that >50% of  
175 communities in all three compartments were dominated by *C. albicans* (defined as >50% relative abundance),  
176 with a progressive decline in fungal Shannon index in oral and lung communities during follow-up (Figure S3).  
177 Nanopore metagenomics of lung samples provided similar bacterial representations to 16S analyses and



178 confirmed high abundance of *C.albicans* detected by ITS sequencing (Figure S3). Thus, our analyses revealed  
179 a pattern of compartment-wide dysbiosis in ICU patients, with progressive decline in diversity and enrichment  
180 for plausible pathogenic bacteria and *C. albicans*. We then sought to understand whether patient-level  
181 variables accounted for baseline or longitudinal dysbiosis.

### 183 Clinical diagnoses and antibiotic exposure correlate with microbial community diversity and composition.

184 We constructed linear regression models with ecological metrics indicative of dysbiosis as outcomes  
185 (baseline Shannon index, obligate anaerobe and respiratory pathogen abundance) and clinical variables as  
186 predictors (Figure S4). History of COPD, immunosuppression and clinical diagnosis of pneumonia showed the  
187 most significant associations with dysbiosis features, e.g. lower Shannon and anaerobe abundance in oral and  
188 lung communities for patients with COPD, and increased pathogen abundance in all three compartments for  
189 patients with history of immunosuppression (Figure S4). History of immunosuppression was also associated  
190 with higher abundance of *C. albicans* in oral and lung samples (Figure S3D). To further explore iatrogenic  
191 forces on microbiota composition, we focused on two common treatments in the ICU: antibiotics and steroids.  
192 We assessed antibiotic usage by i) anaerobic coverage, ii) a numerical scale that included duration, timing and  
193 type,<sup>16</sup> and iii) the Narrow Antibiotic Treatment (NAT) score.<sup>12,17</sup> We quantified steroid use as the daily  
194 equivalent dosage of prednisone in milligrams. Antibiotic usage was associated with Shannon index, anaerobe,  
195 and pathogen abundance in baseline gut samples, with exposure to antibiotics with anaerobic spectrum at  
196 baseline being inversely correlated with anaerobe abundance in all three compartments (Figure S4B). To  
197 explore the effects of antibiotics and steroids over time, we employed mixed linear regression models using  
198 longitudinal samples. In all three compartments, the receipt of anaerobic spectrum antibiotics was associated  
199 with a progressive decrease in obligate anaerobe abundance, without significant effects on pathogen  
200 abundance (Table S2). Notably, antibiotic exposure quantified by the NAT score was also significantly linked to  
201 a reduction in anaerobe abundance and an increase in pathogen abundance within the gut microbiota.  
202 Steroids were associated with decrease in anaerobes in the lungs, but not with changes in abundance of other  
203 microbes in other compartments.

205 Microbial communities in each compartment form distinct clusters of diversity and composition.

206 We next examined the microbial communities independent of clinical variables to capture important  
207 features directly from microbiome data. To understand microbial heterogeneity within compartments, we  
208 leveraged two complementary unsupervised clustering approaches: i) Dirichlet Multinomial Mixture (DMM)  
209 models for 16S data in each compartment (“bacterial DMM clusters”) and for Nanopore metagenomic data in  
210 the lung compartment<sup>18</sup>, and ii) weighted Similarity Network Fusion (SNF)<sup>19</sup> clusters for combined bacterial  
211 (16S) and fungal (ITS) data within each compartment (“bacterial-fungal SNF clusters”).

212 By bacterial DMM clusters, a three-class model offered optimal classification in each compartment, with  
213 striking differences in alpha diversity and composition between clusters (Figure 3A). Cluster 1 in each  
214 compartment had high Shannon index in the range of healthy controls (referred to as High-Diversity cluster),  
215 cluster 3 had low Shannon index (Low-Diversity cluster), and cluster 2 had intermediate diversity (Intermediate-  
216 Diversity cluster). Low-diversity clusters had markedly higher abundance of pathogens and lower abundance of  
217 anaerobes (Figure 3B-C). In cross-compartment comparisons, DMM cluster membership was strongly  
218 associated between oral and lung communities (odds ratio of membership in the Low-Diversity cluster in both  
219 compartments 9.74, 95% confidence interval [5.61-17.29],  $p < 0.0001$ ), whereas lung and gut clusters were less  
220 strongly associated although statistically significant ( $p = 0.015$ , Figure 3D). In longitudinal analyses, cluster  
221 membership showed relative stability for all compartments, with most samples assigned to Low-Diversity  
222 cluster at baseline being assigned to Low-Diversity in the middle interval as well (77% of oral, 80% of lung, and  
223 78% of gut samples, respectively, Figure S5). Nanopore DMM clustering in 130 available lung samples also  
224 showed optimal fit with three total clusters (data not shown). Bacterial-Fungal SNF clustering revealed distinct  
225 communities in each compartment, with a notable cluster in lung samples (cluster 1) with high pathogen  
226 abundance and *C. albicans* dominance (near 100% of fungal sequences abundance) (Figure S6). Thus, our  
227 unsupervised clustering approaches captured broad differences in meta-communities that were not specific to  
228 individual taxa. We next examined how these microbial communities related to host responses and clinical  
229 outcomes.

230  
231 Lung microbiota correlate with systemic host responses.

232 We examined host-microbiota interactions with two independent approaches, a microbiota- and a host-  
233 centric approach. In the microbiota-centric approach, we correlated the top 20 abundant taxa in each  
234 compartment with systemic (plasma) and lung-specific (ETA/BALF supernatants) host response biomarkers.  
235 We found several significant correlations (Figure S7A-C), with typical pathogens (e.g. *Klebsiella*, *Escherichia*-  
236 *Shigella*, *Staphylococcus* genera in the lung compartment) positively correlating with plasma inflammatory  
237 biomarkers (such as sTNFR1 and IL-6 levels), whereas typical oral commensals (e.g. *Rothia*, *Streptococcus*,  
238 *Prevotella* etc.) inversely correlated with plasma sTNFR1 or sRAGE. In cluster comparisons, the bacterial  
239 DMM Low-Diversity cluster in the lungs was significantly associated with higher plasma sTNFR1, sRAGE and  
240 procalcitonin levels (Figure S7D), whereas the Nanopore DMM Low-Diversity cluster was also significantly  
241 associated with higher regional (IL-6 and sRAGE) and systemic biomarkers of injury and inflammation (plasma  
242 IL-6, sTNFR1, sRAGE, Ang-2 and Pentraxin-3, Figure S7E).

243 In the host-centric approach, we applied a widely validated framework of host-response subphenotypes  
244 based on plasma biomarkers.<sup>7,20</sup> With a validated 4-biomarker parsimonious model (using sTNFR1, Ang2,  
245 procalcitonin and bicarbonate levels),<sup>20</sup> we classified individuals at baseline into a hyperinflammatory (22.9%)  
246 vs. a hypoinflammatory (77.1%) subphenotype. We found no significant relationship between host  
247 subphenotypes and DMM microbiota clusters in any compartment (Figure S7G), but hyperinflammatory  
248 patients had higher pathogen abundance in lung communities ( $p=0.04$ ). To further investigate this association,  
249 we stratified patients by pneumonia diagnosis. We discovered that hyperinflammatory patients without  
250 pneumonia had higher pathogen abundance in lung samples compared to hypo-inflammatory patients  
251 ( $p=0.018$ , Figure S7H). These notable associations between lung pathogen abundance and the  
252 hyperinflammatory subphenotype imply that systemic subphenotypes might stem, at least in part, from  
253 undiagnosed pneumonia or respiratory dysbiosis.

#### 254 Lung microbiota clusters predict survival independent of clinical variables and host responses.

256 Comparisons of microbial communities between survivors and non-survivors at 60-days post-ICU  
257 admission showed highly significant differences in alpha diversity in the lungs ( $p<0.0001$ ), as well as higher  
258 obligate anaerobe and lower pathogen abundance in both oral and lung samples (all  $p<0.002$ , Figure S8A-C),

259 but no differences in gut profiles. Additionally, analyses of lung samples stratified by whether they exhibited  
260 gut-origin taxa enrichment (defined as >30% relative abundance) showed markedly worse survival for patients  
261 with gut-origin taxa enrichment ( $p < 0.0001$ , Figure S2E-F).

262 Analyses by bacterial DMM clusters provided further insights with regards to the prognostic value of  
263 each compartment. In both oral and lung compartments, the Low-Diversity clusters were associated with worse  
264 60-day survival in Kaplan-Meier curve analyses, whereas gut clusters had no survival impact (Figure 4A-C).  
265 Notably, the prognostic effects of the Low-Diversity bacterial DMM cluster in the lungs remained significant  
266 after adjustment for age, sex, history of COPD, immunosuppression, severity of illness by SOFA scores and  
267 host-response subphenotypes (adjusted Hazards Ratio-HR= 2.51 [1.26-4.98],  $p = 0.008$ ). Similarly, survival  
268 analysis by the bacterial-fungal SNF lung clusters showed that cluster 1, which had high pathogen and *C.*  
269 *albicans* abundance, also independently predicted worse survival (adjusted HR=2.04 [1.45-2.86],  $p < 0.0001$ ,  
270 Figure 4E). The other bacterial-fungal SNF oral and gut clusters did not impact survival (Figure 4D,F). Thus,  
271 we found evidence that lung microbiota dysbiosis predicted survival beyond the information provided by clinical  
272 predictors, commonly used organ dysfunction indices, and biological subphenotyping.

#### 273 274 Derivation of a dysbiosis index and external validation in patients with COVID-19.

275 Motivated by the robust, independent prognostic impact of microbiota clusters on patient survival, we  
276 next sought to construct predictive models to classify bacterial profiles into the corresponding DMM clusters  
277 within each compartment. Such predictive models could serve as dysbiosis indices beyond the derivation  
278 cohort with our DMM analysis. We used probabilistic graphical modeling (PGM) to predict the DMM clusters in  
279 each compartment based on the abundance of the top 50 taxa and the corresponding Shannon index. By  
280 splitting the dataset in training and testing subsets (80% and 20% of data points, respectively), we developed  
281 separate multinomial regression models for DMM cluster predictions in each compartment (i.e. compartment-  
282 specific Dysbiosis Index), which showed accuracy of 0.76, 0.86 and 0.75 for oral, lung and gut clusters,  
283 respectively. We verified that patients classified in the low diversity clusters by the Dysbiosis Index for the oral  
284 and lung compartments had worse survival, similarly to the DMM-derived clusters.

285 We next applied the derived Dysbiosis Indices to two independent cohorts of hospitalized patients with  
286 COVID-19 pneumonia. In the UPMC-COVID cohort of patients with COVID-19 ARDS on IMV (n=49), the Lung  
287 Dysbiosis Index classified ETA samples into three clusters with significant differences in Shannon index and  
288 bacterial load by qPCR (Figure 5A), but no difference in ETA SARS-CoV-2 viral load by qPCR or 60-day  
289 survival (data not shown). Patients assigned to the low diversity cluster at baseline had higher plasma levels of  
290 sTNFR1 and Ang-2 compared to the high diversity cluster ( $p < 0.05$ , Figure 5B). By individual taxa abundance,  
291 oral commensals (e.g. *Prevotella*, *Veillonella* or *Streptococcus*) were inversely correlated with plasma sTNFR1  
292 and Ang-2, whereas *Klebsiella* abundance was positively correlated (all  $p < 0.05$ ), corroborating the findings of  
293 the cluster analyses relating lung microbiota with prognostically adverse higher levels of systemic biomarkers  
294 of inflammation and endothelial injury.

295 In the MGH-COVID cohort (n=97), we performed metagenomic sequencing in longitudinal lung (ETA for  
296 patients on IMV or expectorated sputum in spontaneously breathing patients) and gut (stool) samples obtained  
297 upon enrollment and then daily up to day 4. We found no significant changes over time in Shannon Index and  
298 anaerobe/pathogen abundance in either compartment on serial samples through day 4. We classified baseline  
299 lung and gut samples by our Dysbiosis Index models, which showed significant differences in Shannon index,  
300 anaerobe and pathogen abundance in each compartment (Figure 5C-D). Importantly, the low diversity cluster  
301 in the lung compartment was strongly associated with COVID-19 pneumonia severity (odds ratio 8.77 [1.75-  
302 67.74], Figure 5E-F), as classified by oxygen support requirements, whereas gut clusters were not. Thus,  
303 application of the Dysbiosis Indices to lung and gut samples of patients with COVID-19 provided similar  
304 findings to the ones obtained in the UPMC-ARF derivation cohort, supporting the predictive value of lung  
305 microbiota profiling.

## 307 **Discussion:**

308 We conducted a longitudinal, integrative assessment of host-microbiota interactions in a large cohort of  
309 ARF patients across three body sites (the oral cavity, lungs, and gut) and up to three time-points in the ICU.  
310 These analyses offered insights into the temporal relationships between patient-level factors, therapeutic  
311 interventions, microbial communities and patient-centered outcomes, which has not been possible in previous

312 smaller scale investigations.<sup>21</sup> The progressive dysbiosis of microbial communities observed in all three body  
313 compartments highlights the impact of critical illness on the global microbiota. We found reduced alpha  
314 diversity and deviation in composition compared to healthy controls at the onset of IMV, with further reduction  
315 in diversity and alterations in composition for patients supported on ventilators over time. Unsupervised  
316 analyses of microbiota composition revealed distinct communities in all three body compartments, yet the lung  
317 microbiome emerged as the strongest independent predictor of important clinical outcomes. We developed  
318 parsimonious models for dysbiosis classifications in each compartment and found that lung dysbiosis was  
319 significantly associated with host-response profiles and clinical severity in patients with COVID-19.

320 The large sample size and granular clinical data in our derivation cohort allowed for detailed  
321 investigation of the relationships between patient-/treatment-related factors with the composition of microbiota.  
322 Clinical diagnoses (e.g., ARDS or pneumonia) and comorbidities explained variation in diversity and  
323 composition at baseline. We detected significant associations between systemic steroid exposure and lung  
324 microbiota composition, a novel finding that warrants validation in other cohorts. Despite the self-evident  
325 biological plausibility of antibiotic pressures on altering the microbiomes of critically ill patients, empirical  
326 evidence to date has been limited.<sup>22-24</sup> Here we modeled antibiotic exposure thoroughly with different  
327 methodologies from prior studies focused on cystic fibrosis or pneumonia,<sup>16,17,25</sup> and studied antibiotic effects  
328 on longitudinal communities and features of dysbiosis. We found that the NAT score and a simple categorical  
329 classification with regards to anaerobic spectrum coverage captured important effects on longitudinal  
330 composition. Recent epidemiologic and molecular evidence supports disruptive effects of anti-anaerobic  
331 antibiotics in gut microbial communities.<sup>24,26</sup> Our data are consistent with the idea that anaerobe-targeting  
332 antibiotics are associated with anaerobic bacteria depletion in the respiratory and the intestinal tracts, and  
333 furthermore our study suggests that such depletion is associated with worse clinical outcome. Therefore, our  
334 results highlight the importance of rational use of anti-anaerobic antibiotics as directed by proper clinical  
335 indications, because such antibiotics can have important yet under-recognized adverse clinical implications.

336 The biogeography of the intubated respiratory tract has been the focus of extensive investigation for  
337 prevention of secondary ventilator-associated pneumonia (VAP).<sup>27,28</sup> Oropharyngeal decontamination with

338 chlorhexidine rinses or the more aggressive selective digestive decontamination (SDD) of the gastrointestinal  
339 tract have been studied for reducing bacterial burden in probable source compartments that seed the LRT  
340 microbiota. While both decontamination approaches are supported by randomized clinical trial evidence  
341 showing efficacy in VAP prevention<sup>29,30</sup>, both approaches also have associated safety concerns,<sup>31,32</sup> leading to  
342 limited uptake of SDD worldwide. Indiscriminate application of chlorhexidine rinses in all patients on IMV may  
343 also deplete commensal organisms from the URT and reduce colonization resistance against pathogens. We  
344 found significant correlations between oral-origin commensal taxa abundance in URT and LRT samples, such  
345 as *Prevotella*, with prognostically favorable, lower levels of plasma inflammatory biomarkers, which may  
346 indicate favorable regulation of innate immunity by such taxa.<sup>33-35</sup> Our comparative analyses between  
347 compartments showed much higher oral-lung than lung-gut similarity, suggesting that the oral cavity serves as  
348 the primary source of microbial seeding for the lungs. However, we found that a small subset of patients had  
349 enrichment for gut-origin commensal or pathogenic organisms in their LRT, which could not be fully accounted  
350 for by URT colonization with similar taxa. Such patients with gut-origin bacteria enrichment in their lungs  
351 (8.1%) had much worse survival than the rest of the cohort, and may represent a subset of patients in whom  
352 gut-to-lung bacterial translocation may have occurred.<sup>36,37</sup> Wider availability of BAL samples to investigate the  
353 alveolar spaces more closely can provide more evidence into the question of gut-to-lung translocation, but our  
354 non-invasive ETA samples showed that such translocation, if present, affects a small subset of patients at least  
355 within the first week of IMV. Therefore, efforts focused on preventing dysbiosis and pathogen colonization in  
356 the URT-to-LRT ecosystem may offer higher biological plausibility for measurable benefits in clinical trials.

357       Unsupervised clustering revealed distinct microbial communities within and across body compartments.  
358 Low-diversity bacterial clusters were enriched with pathogens and depleted in anaerobes in all three  
359 compartments. Membership in the low-diversity cluster was strongly associated between the oral and lung  
360 compartment, suggesting shared patterns of dysbiosis. The overall stability of longitudinal cluster membership  
361 indicated that specific microbial profiles may persist throughout critical illness, influencing the disease  
362 trajectory. Integration of fungal sequencing data further enhanced our view of the microbial communities,  
363 revealing patients who had a “double-hit” of bacterial pathogen enrichment and *C.albicans* dominance in their  
364 communities. We have recently shown that *C.albicans* abundance in the LRT correlates with systemic

365 inflammation and predicts adverse outcome in patients with ARF on IMV.<sup>13</sup> With the current expanded dataset,  
366 we demonstrate that integration of bacterial and fungal data can identify patient subpopulations with inter-  
367 kingdom dysbiosis, who may require different interventions to address both bacterial and fungal dysbiosis.

368 Survival analyses based on microbiota clusters revealed two significant and novel findings. First, in this  
369 comparison of microbiota from three distinct body compartment microbiota for predicting survival in critically ill  
370 patients, the lung microbiome emerged as the most powerful predictor compared to oral or gut microbiota.  
371 Perhaps this finding should not be surprising when studying patients who required IMV for ARF. We had  
372 previously shown that baseline lung microbiota profiles were predictive of survival.<sup>3</sup> We now expand analyses  
373 to three compartments up to three time points during IMV and show that lung microbiota carry the most  
374 predictive signal for survival, both at baseline and also in follow-up samples. Thus, our comparative  
375 assessment of microbiota across body compartments highlights the clinical relevance of lung microbiota  
376 analysis in critical illness and the need for dedicated sampling of the LRT.<sup>38</sup> Second, the prognostic value of  
377 lung microbiota clusters was independent not only from clinical predictors and validated organ dysfunction  
378 metrics, such as the SOFA score, but also from the systemic host-response subphenotypes. Extensive  
379 evidence has established the prognostic value and generalizability of plasma biomarker-based subphenotyping  
380 of patients with ARF.<sup>8,39</sup> Our adjusted Cox proportional hazards models revealed significant hazards ratios for  
381 the Low-Diversity lung cluster, when analyzed using both the bacterial DMM and bacterial-fungal SNF  
382 methods. Beyond the significant taxa-biomarker associations we observed, the survival analyses demonstrated  
383 that lung microbiota may influence patient outcome in ways that are not captured by current host-response  
384 subphenotyping approaches. An integrative, host- and lung microbiome-aware subphenotyping framework may  
385 thus augment our ability to better prognosticate and target therapeutic interventions in ARF.

386 Our study has several limitations. First, we mainly focused on bacterial and fungal components of the  
387 microbiome, and thus could not assess the role of the virome, especially with regards to respiratory RNA  
388 viruses. The consistent pattern of results relating elements of the bacterial microbiome to host response and  
389 illness severity in the COVID-19 cohorts supports the generalizability of our findings, although we could not  
390 investigate contributions from individual viruses. The observational nature of our study prevents us from



391 establishing causality between the microbiome and clinical outcomes, which could be addressed by future  
392 interventional studies or animal modeling with microbiome manipulation. Longitudinal sample availability was  
393 limited by informative censoring, as patients with rapid decline and early death or those with rapid improvement  
394 and liberation from IMV would not contribute follow-up samples in the middle and late intervals. We aimed to  
395 mitigate some of these right censoring biases with mixed linear regression models, but our longitudinal  
396 analysis findings should be interpreted with caution and considered as applicable to patients who remain on  
397 IMV for the first 1-2 weeks of critical illness. For patient safety and practical purposes of subject participation in  
398 our observational research study, we relied on non-invasive biospecimens (ETA) for LRT microbiota profiling,  
399 as opposed to reference standard BAL.<sup>38</sup> Our non-invasive approach allowed us to enroll a large cohort of LRT  
400 specimens, follow serial samples over time, and is congruent with clinical practice guidelines for VAP  
401 diagnosis.<sup>40</sup> However, we may have missed important microbiota variability closer to the alveolar space,  
402 including a stronger signal of gut-to-lung microbiota translocation.<sup>37</sup> Finally, we had a smaller effective sample  
403 size for gut microbiota analysis, which may have limited our ability to identify prognostic variation within the gut  
404 compartment.

405 In conclusion, our study provides novel insights into the predictive value of microbiota clusters derived  
406 from different body compartments in critically ill patients. The lung microbiome emerged as the most powerful  
407 predictor of survival, surpassing the oral and gut microbiota. These findings emphasize the clinical relevance of  
408 investigating the lung microbiota and highlight its potential as a prognostic marker in critical illness. Moreover,  
409 our study underscores the importance of considering organ-specific microbial communities in critical care  
410 settings and expands our understanding of the microbiome's role in determining patient outcomes. Further  
411 research in this area has the potential to shape clinical decision-making and facilitate the development of  
412 personalized medicine strategies for critically ill patients.

## 413 **Online Methods**

414 UPMC-ARF cohort: Following admission to the ICU at UPMC (Pittsburgh, PA, USA) and obtaining informed  
415 consent from patients or their legally authorized representatives (University of Pittsburgh IRB protocol  
416 STUDY19050099), we collected baseline research biospecimens within 72hrs from intubation. We collected  
417 blood for separation of plasma, oropharyngeal (oral) swabs to profile upper respiratory tract (URT) microbiota,  
418 endotracheal aspirates (ETA) for LRT (lung) microbiota and host biomarker measurements, and rectal swabs  
419 or stool samples for gut microbiota analyses. We also captured leftover bronchoalveolar lavage fluid (BALF)  
420 from clinically indicated bronchoscopies, when available. We repeated research biospecimen sampling  
421 between days 3-6 (middle interval) and days 7-12 (late interval) post enrollment for subjects who remained in  
422 the ICU. No patients in the UPMC-ARF cohort were known to be infected by SARS-CoV-2 at the time of  
423 enrollment.

424 UPMC-COVID cohort: Following admission to the ICU and obtaining informed consent from patients or their  
425 legally authorized representatives (University of Pittsburgh IRB protocol STUDY19050099), we collected  
426 baseline research biospecimens (ETA and blood) within 72hrs from intubation. We repeated research  
427 biospecimen sampling between days 3-6 (middle interval) and days 7-12 (late interval) post enrollment for  
428 subjects who remained in the ICU, as per the UPMC-ARF protocol. All patients were known to be infected by  
429 positive SARS-CoV-2 qPCR prior to enrollment.

430 MGH-COVID cohort: From April 2020 to May 2021, we prospectively enrolled 97 hospitalized patients aged  
431  $\geq 18$  years with confirmed COVID-19 at the Massachusetts General Hospital (Boston, MA, USA) to a  
432 longitudinal COVID-19 disease surveillance study.<sup>15</sup> The Study protocol #2020P000804 was approved by the  
433 Mass General Brigham IRB. All participants or their healthcare proxy provided written informed consent to  
434 participate. Patients were categorized as having severe COVID-19 if they required admission to the intensive  
435 care unit with acute respiratory failure (the need for oxygen supplementation  $\geq 15$  liters per minute (LPM), non-  
436 invasive positive pressure ventilation, or mechanical ventilation) or other organ failure (such as shock requiring  
437 vasopressors). Otherwise, they were categorized as having moderate COVID-19. Expecterated sputum, ETA  
438 or fresh stool was collected and refrigerated at 4°C until aliquoting/freezing at -80°C (typically within 4 hours of  
439 collection) from adult patients enrolled in the prospective biospecimen collection study. Participants were able

440 to provide samples as frequently as once daily for up to four days, as well as declining donation on any given  
441 day (while remaining in the study).

442 Healthy Controls: To contextualize the findings on microbiota from critically-ill patients with what is expected for  
443 the healthy respiratory and gastrointestinal tract, we also included data from 24 healthy volunteers who had  
444 contributed URT and LRT microbiome data in a previously published cohort (Lung HIV Microbiome Project –  
445 University of Pittsburgh IRB STUDY19060243),<sup>41</sup> as well as stool from 15 healthy donors for fecal microbiota  
446 transplantation (University of Pittsburgh IRB - STUDY20060312).<sup>11</sup> We designated these healthy volunteers as  
447 Healthy Controls.

448 Clinical data recording: A consensus committee reviewed clinical and radiographic data and performed  
449 retrospective classifications of the etiology and severity of acute respiratory failure without knowledge of  
450 microbiome sequencing or biomarker data. We retrospectively classified subjects as having ARDS per  
451 established criteria (Berlin definition), being at risk for ARDS because of the presence of direct (pneumonia or  
452 aspiration) or indirect (e.g., extrapulmonary sepsis or acute pancreatitis) lung-injury risk factors although  
453 lacking ARDS diagnostic criteria, having acute respiratory failure without risk factors for ARDS, or having  
454 acute-on-chronic respiratory failure. We followed patients prospectively for cumulative mortality and ventilator-  
455 free days (VFDs) at 30 days, as well as survival up to 60 days from intubation.

456 We systematically reviewed administered antibiotic therapies since hospital admission and recorded the  
457 antibiotic exposure for each subject according to the following three metrics:

- 458 1. Anaerobic coverage (yes/no): whether antibiotics with anaerobic coverage were given on the day of  
459 sampling.
- 460 2. The Antibiotic Exposure score by Zhao et al <sup>16</sup>: a numerical scale with antibiotic weighting based on  
461 dosing duration, timing of administration relative to sample collection and antibiotic type and route of  
462 administration. We utilized the convex increasing weighting scheme and modeled the antibiotic  
463 exposure from hospital admission until day of sampling.
- 464 3. The Narrow Antibiotic Treatment (NAT) score developed for community-acquired pneumonia treatment  
465 studies <sup>17,25</sup>. We calculated the daily NAT score from -5 days from sampling to post 10 days after  
466 sampling on day 1.

467

468 Research Sample Collection

469           Within the first 48 hours of intubation (baseline time-point), we collected a posterior oropharyngeal  
470 (oral) swab via gentle swabbing the posterior oropharynx next to the endotracheal tube with a cotton tip swab  
471 for 5 secs, and an endotracheal aspirate (ETA) via suctioning secretions from the endotracheal tube with the  
472 in-line suction catheter and without breaking seal in the ventilatory circuit.<sup>1,4</sup> Rectal swabs were collected  
473 according to a standard operating procedure (i.e., placing the patient in a lateral position, inserting the cotton  
474 tip of the swab into the rectal canal, and rotating the swab gently for 5 s), unless clinical reasons precluded  
475 movement of the patient (e.g., severe hemodynamic or respiratory instability). Stool samples were collected  
476 when available, either by taking a small sample from an expelled bowel movement (before cleaning of the  
477 patient and disposal of the stool) or from a fecal management system (rectal tube) placed for management of  
478 diarrhea and liquid stool collection. We also collected simultaneous blood samples for centrifugation and  
479 separation of plasma. Samples were delivered to the processing laboratory within minutes from acquisition,  
480 and then aliquoted and stored in -80C until conduct of experiments. For samples that underwent host DNA  
481 depletion for Nanopore sequencing, an aliquot remained in 4C for processing before freezing for up to 72hrs  
482 from acquisition. ETA Samples obtained from COVID-19 subjects inactivated by 4-fold dilution in DNA/RNA  
483 Shield (Zymo Research) under biosafety level 2+ conditions and then stored at -80°C. For patients who  
484 remained intubated in the ICU, we collected follow-up samples at a middle time-point (days 3-6) and a late  
485 follow-up interval (days 7-11 post-intubation).

486           For Healthy Controls, an oral wash and BAL sample were collected with a standardized protocol.<sup>41</sup>  
487 Subjects were asked to fast and refrain from smoking for at least 12hrs before sample collection. Oral washes  
488 were performed by having participants gargle with 10 ml sterile 0.9% saline immediately before bronchoscopy.  
489 BAL was performed according to standardized procedures developed to minimize oral contamination.  
490 Participants gargled with an antiseptic mouthwash (Listerine) immediately before topical anesthesia. The  
491 bronchoscope was then inserted through the mouth and advanced to a wedge position quickly and without use  
492 of suction. BAL was performed in the right middle lobe or lingula up to a maximum of 300 ml 0.9% saline.

493 Healthy donors of stool for fecal microbiota transplant collected a stool sample in a specialized container and  
494 brought the stool sample on the day of collection to the processing lab.

495

#### 496 *Laboratory Analyses*

497 Microbiome assays in UPMC cohorts: From all available oral swabs, ETAs, left over BALF, rectal swabs and  
498 stool samples, we extracted genomic DNA and performed quantitative PCR (qPCR) of the V3-V4 region of the  
499 16S rRNA gene to obtain the number of gene copies per sample, as a surrogate for bacterial load. From a  
500 separate aliquot of extracted DNA from oral swabs, ETA, rectal swabs and stool samples, we performed  
501 amplicon sequencing for bacterial DNA (16S-Seq of the V4 hypervariable region) and fungal DNA (ITS) on the  
502 Illumina MiSeq platform at University of Pittsburgh Center for Medicine and the Microbiome laboratories.<sup>3,42</sup>

503 We used extensive experimental negative controls in all processing steps to rule out contamination, as well as  
504 mock microbial community positive controls (Zymo) to ensure target amplification success. We processed  
505 derived 16S sequences with a custom Mothur-based pipeline and performed analyses at genus level. From a  
506 random subset of 130 available ETA samples, we performed metagenomic Nanopore sequencing (following  
507 human DNA depletion) with a rapid PCR barcoding kit (SQK-RPB004) on the MinION device (Oxford  
508 Nanopore Technologies-ONT, Oxford, UK) for five hours.<sup>43,44</sup> We analyzed microbial metagenomic sequences  
509 with the EPI2ME platform (ONT) and the “What’s In My Pot” [WIMP] workflow to quantify abundance of  
510 microbial species.<sup>45</sup> We filtered FASTQ files with a mean quality (q-score) below a minimum threshold of 7.

511 Host-response assays: We measured 10 plasma biomarkers of tissue injury and inflammation with custom  
512 Luminex multi-analyte panels from plasma samples and ETA supernatants, when available. Specifically, we  
513 used a 10-plex Luminex panel (R&D Systems, Minneapolis, MI, United States) to measure interleukin(IL)-6, IL-  
514 8, IL-10, soluble tumor necrosis factor receptor 1 (sTNFR1), suppressor of tumorigenicity-2 (ST2), fractalkine,  
515 soluble receptor of advanced glycation end-products (sRAGE), angiopoietin-2, procalcitonin and pentraxin-3.<sup>7</sup>

516 Microbiome assays in MGH-COVID cohort: Samples were extracted and sequenced at Baylor College of  
517 Medicine according to their standard established platforms. DNA was prepared for sequencing using the  
518 Illumina Nextera XT DNA library preparation kit. All libraries were sequenced with a target of 3GB output at  
519 2x150bp read length using the Illumina NovaSeq platform, as previously described.<sup>15</sup>

520  
521 Quantification and statistical analysis.

522 We performed non-parametric comparisons for continuous (described as median and interquartile  
523 range – IQR) and categorical variables between clinical groups (Wilcoxon and Fisher’s exact tests,  
524 respectively). For microbial community profiling, we included samples that produced >300 high quality  
525 microbial reads for both 16S-Seq and Nanopore sequencing. We performed alpha diversity (Shannon index)  
526 calculations for each available sample, and then conducted between group comparisons of alpha diversity with  
527 non-parametric tests to draw inferences on systematic differences of alpha diversity between groups as a  
528 measure of relative community fitness.<sup>1</sup> We conducted beta diversity analyses (Manhattan distances, analyzed  
529 via permutation analysis of variance and visualized via principal coordinates analyses) with the R *vegan* and  
530 *mia* packages.<sup>46</sup> We examined for differentially abundant taxa between groups following centered log-ratio  
531 (CLR) transformations with the *limma* package to fit weighted linear regression models, perform tests based on  
532 an empirical Bayes moderated *t*-statistic and obtain False Discovery Ratio corrected p-values.

533 We then examined the discovered bacterial taxa at genus level and classified them by two different  
534 classification schemes with clinical relevance<sup>12</sup>:

535 A. By oxygen requirements for bacterial metabolism:

- 536 1. Obligate aerobes (referred to throughout as aerobes): bacteria that require oxygen to grow  
537 and survive, as they use oxygen as final electron acceptor in their respiratory chain.
- 538 2. Obligative anaerobes (referred to throughout as anaerobes): bacteria that are unable to  
539 grow in the presence of oxygen, as they are unable to use oxygen as a final electron  
540 acceptor and are killed in the presence of oxygen.
- 541 3. Facultative anaerobes: bacteria that can grow in the presence or absence of oxygen. They  
542 can use both aerobic and anaerobic respiration, depending on the availability of oxygen in  
543 their environment, switching from aerobic to anaerobic metabolism.
- 544 4. Microaerophiles: bacteria that require a low level of oxygen to grow and survive, as they can  
545 grow at oxygen concentrations lower than those required by obligate aerobes but higher  
546 than those tolerated by obligate anaerobes.

- 547 5. Variable: genera that included both aerobes and anaerobes and could not be classified  
548 further with confidence.
- 549 6. Unclassifiable: taxa that were not classified at the genus or family level with confidence to  
550 allow assessment of their metabolic needs.

551 B. By pathogenicity for LRT infections:

- 552 1. Common respiratory pathogens: bacteria considered to be typical pathogens when isolated  
553 in LRT microbiologic cultures.
- 554 2. Oral-origin commensal bacteria: bacterial taxa that have been characterized as typical  
555 members of the lung microbiome in health and originate from the oral cavity.
- 556 3. Other: taxa with unclear clinical significance that do not fall into categories B1 or B2 above.

557 To agnostically examine our samples for distinct clusters of microbial composition (“metacomunities”),  
558 we applied unsupervised Dirichlet multinomial models (DMMs) with Laplace approximations<sup>18</sup> to define the  
559 optimal number of clusters in our dataset, and then examined for associations with clinical parameters and  
560 outcomes. To synthesize bacterial and fungal data within each compartment, as well as bacterial profiles  
561 across different compartments, we used the weighted Similarity Network Fusion function.<sup>19</sup> We classified  
562 subjects into a hyper- vs. hypo-inflammatory subphenotype based on predictions from a parsimonious logistic  
563 regression model utilizing plasma levels of sTNFR1, Ang-2 and procalcitonin (research biomarkers measured  
564 with Luminex panel), as well as serum bicarbonate levels measured during clinical care.

565 We followed patients prospectively and constructed Kaplan-Meier curves and Cox-proportional hazard  
566 models for 60-day survival, adjusted for the predictors of age and sex, as well as plausible confounders of  
567 microbiome associations diagnosis based on our findings (history of COPD, history of Immunosuppression),  
568 severity of illness as per the SOFA score, and host-response subphenotypes. To examine for the impact of  
569 mechanical ventilation, steroids and antibiotics pressure on longitudinal microbiota profiles, we constructed  
570 mixed regression models with random patient intercepts and adjusted for the number of days post-intubation  
571 that each sample was taken (as a proxy for the exposure to the hyperoxic environment of the ventilator) and  
572 the antibiotic exposure and steroids metrics by the day of sampling. We performed all statistical analyses in R  
573 v.4.2.0.<sup>47</sup>

574 Following derivation of the DMM clusters in each compartment of the UPMC-ARF cohort and  
575 demonstration of significant associations with patient outcomes, we proceeded to develop multinomial logistic  
576 regression models for prediction of classification of bacterial 16S profiles from new samples into predicted  
577 cluster assignments. We considered these new classification models as a Dysbiosis Index for each  
578 compartment. To develop these models in each compartment (oral, lung and gut), we used probabilistic  
579 graphical modeling (PGM)<sup>48</sup> by considering the 50 most abundant taxa in each compartment along with the  
580 Shannon Index. We divided the samples of each compartment into two random subsets: 80% of data points for  
581 training and 20% for testing. The training set was used to generate a PGM using the FCI-MAX algorithm with  
582 Alpha of 0.1 to examine which variables (50 taxa abundance and Shannon Index) were associated with the  
583 cluster assignments in each compartment. The variables that appeared in the Markov blanket of the DMM  
584 cluster assignment variable were used to create a multinomial logistic regression (MLR) model to predict the  
585 cluster assignment of future samples. The MLR model equations were written as follows for the different  
586 cluster assignments (Low, Intermediate and High Diversity):

587 Model equations

$$588 \ln \left( \frac{P(\text{Intermediate})}{P(\text{HighDiversity})} \right) = b_{10} + b_{11} \cdot f_1 + \dots + b_{1n} \cdot f_n \quad \text{Equation 1}$$

$$590 \ln \left( \frac{P(\text{LowDiversity})}{P(\text{HighDiversity})} \right) = b_{20} + b_{21} \cdot f_1 + \dots + b_{2n} \cdot f_n \quad \text{Equation 2}$$

592  $f$ : feature

593  $b_1$  &  $b_2$  are model coefficients

594 By rewriting the equations, we get the following:

$$596 \frac{P(\text{Intermediate})}{P(\text{HighDiversity})} = e^{(b_{10} + b_{11} \cdot f_1 + \dots + b_{1n} \cdot f_n)} \quad \text{Equation 3}$$

$$598 \frac{P(\text{LowDiversity})}{P(\text{HighDiversity})} = e^{(b_{20} + b_{21} \cdot f_1 + \dots + b_{2n} \cdot f_n)} \quad \text{Equation 4}$$

600 We rewrote the names of the model parameters as :

$$601 P(\text{HighDiversity}) = P(H)$$

$$602 P(\text{Intermediate}) = P(I)$$

$$603 P(\text{LowDiversity}) = P(L)$$

$$604 e^{(b_{10} + b_{11} \cdot f_1 + \dots + b_{1n} \cdot f_n)} = X$$

$$605 e^{(b_{20} + b_{21} \cdot f_1 + \dots + b_{2n} \cdot f_n)} = Y$$

606 We know that  $P(H) + P(I) + P(L) = 1$  Equation 5



609 Then  $P(H) = 1 - P(I) - P(L)$  **Equation 6**

610  
611 From **Equation 3 and 4**

612  
613 
$$P(I) = X P(H)$$
$$P(H) = \frac{P(L)}{Y}$$

614  
615  
616 Substituting in **Equation 6**

617  
618 
$$\frac{P(L)}{Y} = 1 - X \frac{P(L)}{Y} - P(L)$$
$$\frac{P(L)}{Y} + X \frac{P(L)}{Y} + P(L) = 1$$
$$P(L) \left[ \frac{1}{Y} + \frac{X}{Y} + 1 \right] = 1$$
$$P(L) \left[ \frac{1 + X + Y}{Y} \right] = 1$$
$$P(L) = \left[ \frac{Y}{1 + X + Y} \right]$$
$$P(H) = \left[ \frac{1}{1 + X + Y} \right]$$
$$P(I) = \left[ \frac{X}{1 + X + Y} \right]$$

622  
623  
624  
625  
626  
627 The predicted cluster is the one with the highest probability. For example, if  $\max(P(H), P(I), P(L)) = P(I)$ ,  
628 then the predicted cluster is  $P(I)$

629  
630 The Intercepts and co-efficients for the MLR models for each compartment are provided below.

Oral		
$f$	$b_1$	$b_2$
Intercept	8.124887	13.323657
ShannonIndex	-1.57054	-2.79173
Actinomyces	0.4883585	0.1975639
Capnocytophaga	0.1550266	-0.2497556
Fusobacterium	0.04705918	-0.49428753
Granulicatella	0.03521261	-0.22396119
Leptotrichia	-0.5982385	-0.6815710
Parvimonas	-0.8593016	-0.6830944
Porphyromonas	-0.7968399	-0.4426564
Prevotellaceae_uncl	-0.3983984	-1.9055700
Stomatobaculum	-0.5966283	-1.3445377

631

Lung		
$f$	$b_1$	$b_2$
Intercept	6.091456	13.161966
ShannonIndex	-2.235179	-3.955922
Streptococcus	0.08810083	-0.30461314
Veillonella	0.27052525	0.04224102

Peptostreptococcus	-0.02538055	0.50470722
Porphyromonas	-0.520896	-1.387346
Selenomonas	-0.5639481	-1.2279826
Alloprevotella	-0.4193465	-1.0781599
Leptotrichia	-0.09918638	-1.16197619
Neisseriaceae_uncl	-0.430702	-1.654160

<b>Gut</b>		
<i>f</i>	<i>b</i> <sub>1</sub>	<i>b</i> <sub>2</sub>
Intercept	-0.7901505	4.5913451
ShannonIndex	2.104042	-1.017060
Atopobium	1.0404839	0.1382178
Streptococcus	-0.1680732	0.2080845
Enterococcus	-0.04209851	0.38397607
Faecalibacterium	-0.8249428	-0.9945793
Fenollaria	0.4178598	-0.5862931
Alistipes	-1.3291409	-0.6846156
Lachnospiraceae_uncl	-1.1289312	-0.7073528

We tested the MLR model using three datasets: The 20% testing set for estimating model accuracy, and the ALIR-COVID samples and the MGH-COVID samples for examining associations between the Dysbiosis Index with clinical variables and endpoints.

Applications of the MLR models (Dysbiosis Index) in the three compartments showed the following accuracy statistics (95% confidence intervals) for prediction of the DMM clusters:

Oral Dysbiosis Index: 0.76 (0.65-0.85)

Lung Dysbiosis Index: 0.86 (0.76-0.93)

Gut Dysbiosis Index: 0.75 (0.60-0.86)

643 **Acknowledgements:**

644 The authors wish to thank the patients and patient families that have enrolled in the University of Pittsburgh  
645 Acute Lung Injury Registry. We also thank the physicians, nurses, respiratory therapists and other staff at the  
646 University of Pittsburgh Medical Center Presbyterian, Shadyside and East Hospitals intensive care units for  
647 assistance with coordination of patient enrollment and collection of patient samples. We would like to thank the  
648 laboratory personnel at the Center for Medicine and the Microbiome at the University of Pittsburgh for  
649 assistance with processing clinical samples. We acknowledge the contributions of Nameer Al-Yousif, MD,  
650 Michael Lu, MD, Grace Lisius MD, and Caitlin Shaefer, MPH who participated in clinical data extractions for  
651 specific components of the databases of the UPMC-ARF and UPMC-COVID cohorts. We also thank the  
652 Massachusetts General Hospital Translational and Clinical Research Center (TCRC) for their support of the  
653 project and the assembly of the MGH-COVID cohort.

654 **Ethics approval and consent to participate:** The University of Pittsburgh Institutional Review Board (IRB)  
655 approved the protocol for the UPMC-ARF and UPMC-COVID cohorts (STUDY19050099). We obtained written  
656 or electronic informed consent by all participants or their surrogates in accordance with the Declaration of  
657 Helsinki. For the MGH-COVID cohort, the Study protocol #2020P000804 was approved by the Mass General  
658 Brigham IRB. For the healthy controls, the University of Pittsburgh IRB approved the study protocols  
659 (STUDY19060243 for respiratory biospecimens and STUDY20060312 for stool biospecimens). All participants  
660 or their healthcare proxy provided written informed consent to participate.

662  
663 **Consent for publication:** We obtained necessary patient/participant consent and the appropriate institutional  
664 forms have been archived. Any patient/participant/sample identifiers included were not known to anyone  
665 outside the research group so cannot be used to identify individuals.

666  
667 **Data and code availability:**

668 Sequencing data collected for the study have been deposited to the Sequencing Resource Archive, through  
669 the following Accession numbers:

670 -PRJNA595346 for 16S data of UPMC-ARF and UPMC-COVID cohorts (477 records released and remainder  
671 to be released upon publication with Temporary Submission ID SUB13319619),  
672 -PRJNA726955 for ITS data of UPMC-ARF cohort,  
673 -PRJNA554461 for Nanopore data of UPMC-ARF cohort,  
674 -PRJNA940725 for 16S data of the Healthy Controls,  
675 -PRJNA976404 for Metagenomic data of the MGH-COVID cohort.  
676 Primary code and de-identified data for replication of analyses will be available on the github repository  
677 (<https://github.com/MicrobiomeALIR/MultiCompartmentMicrobiome>) upon acceptance of the manuscript for  
678 publication. Any additional information required to reanalyze the data reported in this paper is available from  
679 the lead contact upon request.

680

681

682

**Table 1:** Baseline characteristics of enrolled mechanically ventilated patients in the UPMC-ARF cohort, stratified by 60-day mortality. We compared continuous variables with non-parametric Wilcoxon tests and categorical variables with Fisher's exact tests between the three groups. Statistically significant differences ( $p < 0.05$ ) are highlighted in bold.

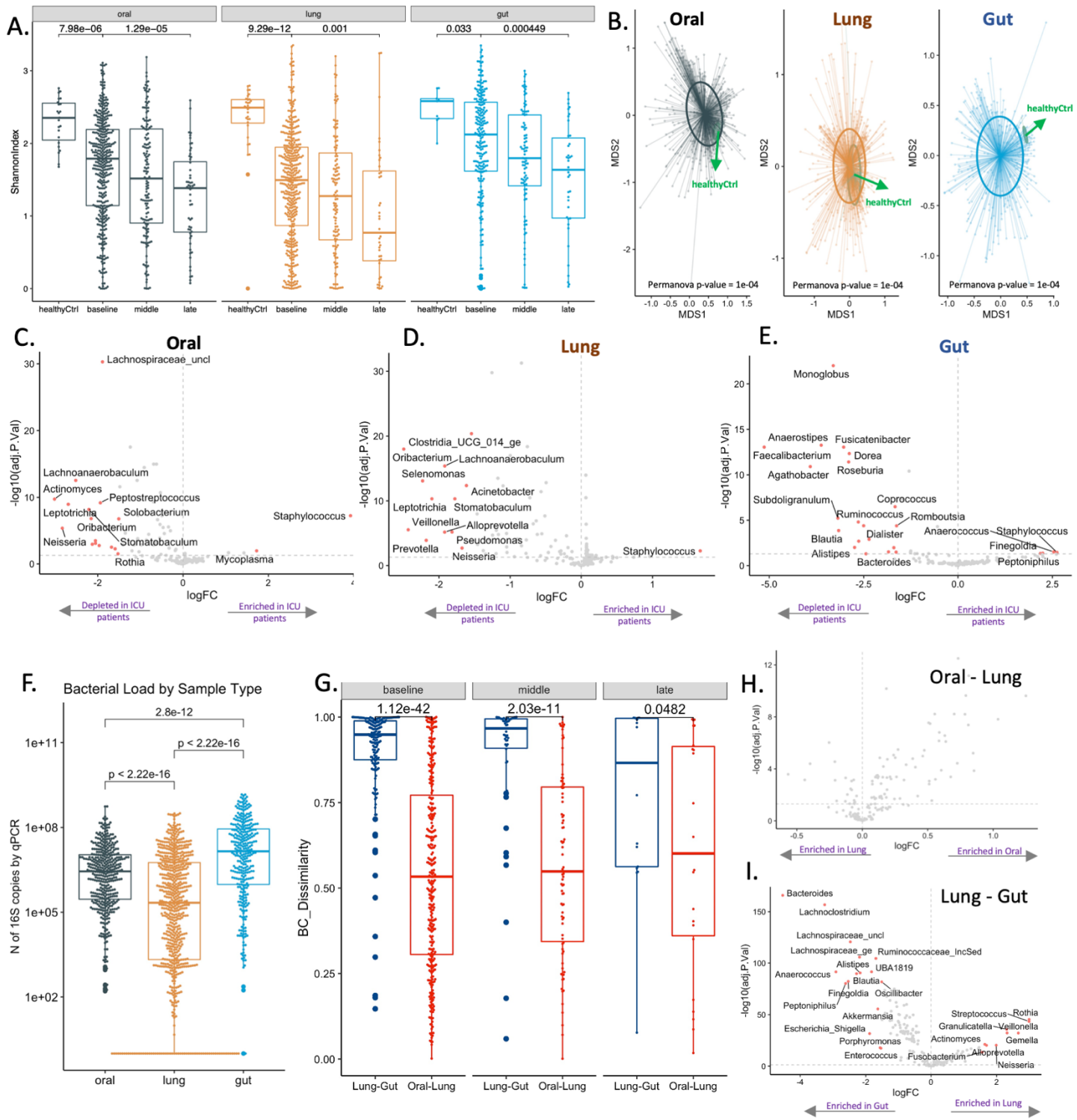
	All	Survivors	Non-Survivors	p
N	479	350	129	
Age, years (median [IQR])	59.6 [46.7, 68.7]	57.1 [44.1, 67.1]	65.3 [55.8, 72.2]	<0.01
Men, n (%)	256 (54.4)	180 (52.6)	76 (58.9)	0.26
Whites, n (%)	425 (90.2)	307 (89.8)	118 (91.5)	0.67
BMI (median [IQR])	29.4 [25.5, 36.0]	29.6 [25.5, 35.7]	28.6 [25.3, 36.6]	0.98
COPD, n (%)	104 (22.1)	75 (21.9)	29 (22.5)	1.00
Diabetes, n (%)	168 (35.7)	122 (35.7)	46 (35.7)	1.00
Alcohol use, n (%)	84 (17.9)	60 (17.5)	24 (18.9)	0.84
Immunosuppression, n (%)	105 (22.3)	71 (20.8)	34 (26.4)	0.24
ARDS, n (%)	117 (25.2)	81 (24.0)	36 (28.1)	0.23
WBC (median [IQR])	12.0 [8.7, 16.8]	11.4 [8.1, 15.8]	14.4 [10.1, 18.7]	<0.01
Creatinine (median [IQR])	1.2 [0.8, 2.3]	1.1 [0.8, 2.0]	1.6 [0.9, 2.5]	0.01
Plateau Pressure (median [IQR])	20.0 [16.0, 25.0]	19.0 [16.0, 24.0]	22.0 [18.0, 27.0]	<0.01
PaO <sub>2</sub> :FiO <sub>2</sub> ratio (median [IQR])	164.0 [117.0, 206.0]	168.0 [121.5, 211.0]	157.0 [108.0, 205.0]	0.04
SOFA scores (median [IQR])	6.0 [4.0, 9.0]	6.0 [4.0, 8.0]	8.0 [5.0, 10.0]	<0.01
LIPS score (median [IQR])	5.5 [4.0, 6.5]	5.0 [4.0, 6.5]	6.0 [5.0, 7.5]	<0.01
Hypoinflammatory subphenotype, n (%)	344 (75.6)	254 (77.4)	90 (70.9)	0.18
VFD (median [IQR])	22.0 [13.0, 25.0]	23.0 [20.0, 25.2]	0.0 [0.0, 19.0]	<0.01

Abbreviations: IQR: Interquartile Range; BMI: body mass index; COPD: chronic obstructive pulmonary disease, LIPS: lung injury prediction score; WBC: white blood cell count; PaO<sub>2</sub>: partial pressure of arterial oxygen; FiO<sub>2</sub>: Fractional inhaled concentration of oxygen; SOFA: sequential organ failure assessment; VFD: ventilator free days; ARDS: acute respiratory distress syndrome.

695 **Figures:**

696 **Figure 1. Ecological features of dysbiosis in three body compartments in critically ill patients. A.**

697 Samples from critically ill patients had significantly lower alpha diversity (Shannon index) compared to  
698 corresponding healthy control samples in each compartment ( $p < 0.001$ ), with further decline of Shannon index  
699 over time in longitudinal samples ( $p < 0.001$ ). B. Baseline samples from critically ill patients had markedly  
700 significant differences in beta diversity from healthy controls (permutational analysis of variance [permanova]  
701  $p$ -values  $< 0.001$ ). C-E. Taxonomic composition comparisons with the *limma* package showed high effect sizes  
702 and significance thresholds (threshold of log<sub>2</sub>-fold-change [log<sub>2</sub>FC] of centered-log-transformed [CLR]  
703 abundances  $> 1.5$ ; Benjamini-Hochberg adjusted  $p$ -value  $< 0.05$ ) showed depletion for multiple commensal taxa  
704 in critically ill patients samples, with significant enrichment for *Staphylococcus* in oral and lung samples, and  
705 *Anaerococcus* and *Enterococcus* in gut samples (significant taxa shown in red in the volcano plots). F. Lung  
706 samples had lower bacterial burden compared to oral and gut samples by 16S qPCR (all  $p < 0.001$ ). G. Oral  
707 and lung samples had higher compositional similarity (Bray-Curtis indices) compared to lung and gut samples  
708 in the baseline and middle interval ( $p < 0.001$ ). H-I: Taxonomic comparisons between compartments revealed  
709 that no specific taxa were systematically different between oral and lung microbiota (H), whereas in gut-lung  
710 comparisons, lung communities were enriched for typical respiratory commensals (e.g. *Rothia*, *Veillonella*,  
711 *Streptococcus*) and gut communities for gut commensals (e.g. *Bacteroides*, *Lachnoclostridium*,  
712 *Lachnospiraceae*) (I).



713

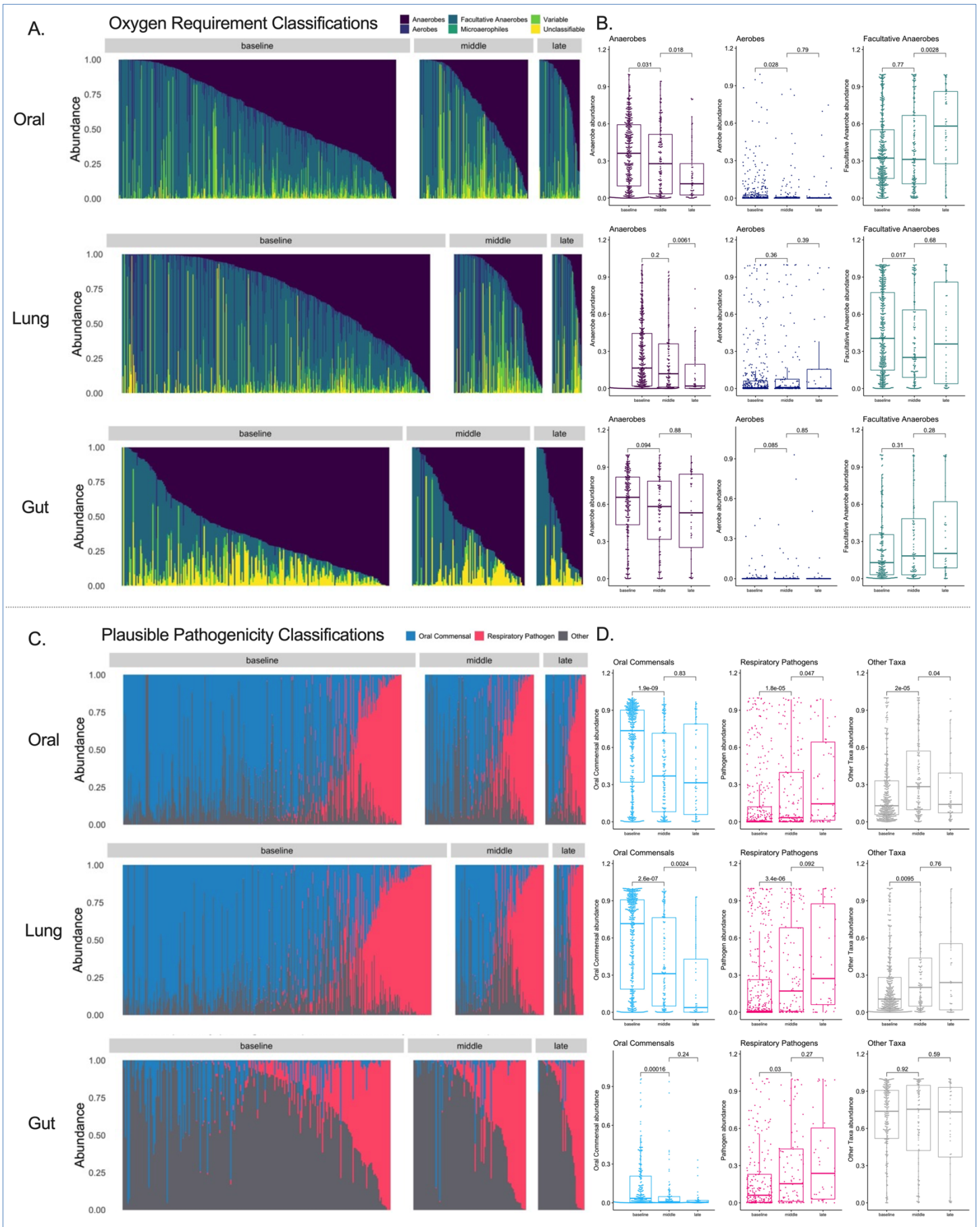
714

715

716

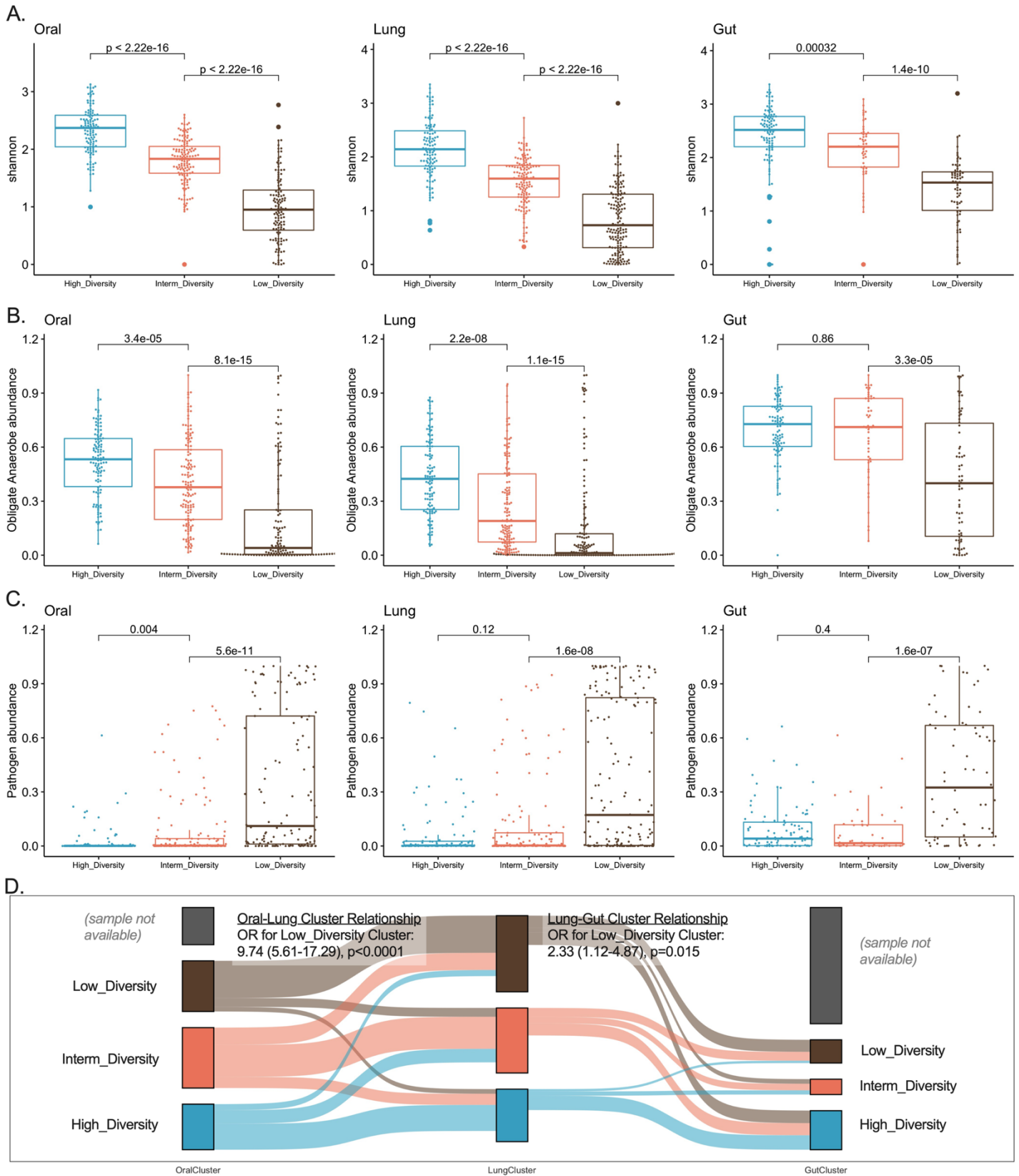
717 **Figure 2: Longitudinal analysis of bacterial composition showed a progressive loss of obligate**  
718 **anaerobes in oral and lung communities as well as enrichment for recognized respiratory pathogens in**  
719 **all three compartments.** Top Panels (A-B): Relative abundance barplots for oral, lung and gut samples with  
720 classification of bacterial genera by oxygen requirement into obligate anaerobes (anaerobes), aerobes,  
721 facultative anaerobes, microaerophiles, genera of variable oxygen requirement and unclassifiable.  
722 Comparisons of relative abundance for the three main categories of bacteria (obligate anaerobes, aerobes and  
723 facultative anaerobes) by follow-up interval (baseline, middle and late). Data in boxplots (B) are represented as  
724 individual values with median values and interquartile range depicted by the boxplots with comparisons  
725 between intervals by non-parametric tests. Bottom Panels (C-D): Relative abundance barplots for oral, lung  
726 and gut (F) samples with classification of bacterial genera by plausible pathogenicity into oral commensals,  
727 recognized respiratory pathogens and “other” category. Comparisons of relative abundance for these  
728 categories of bacteria by follow-up interval (baseline, middle and late) in boxplots (D).





730 **Figure 3: Unsupervised clustering approaches revealed differences in bacterial alpha diversity and**  
731 **composition in three body compartments of critically ill patients.** Panels A-D demonstrate bacterial  
732 Dirichlet Multinomial Mixture (DMM) modeling results for each compartment separately. DMM clusters had  
733 significant differences in alpha diversity (A) and composition (obligate anaerobe abundance in shown in panel  
734 B and pathogen abundance shown in panel C), with cluster 3 in each compartment showing very low Shannon  
735 Index and enrichment for pathogens (Low-Diversity cluster). Oral and lung cluster assignments were strongly  
736 associated (Odds ratio for assignment to the Low-Diversity cluster: 9.74 (5.61-17.29),  $p < 0.0001$ ), whereas lung  
737 and gut cluster assignments were less strongly but significantly associated (panel D).

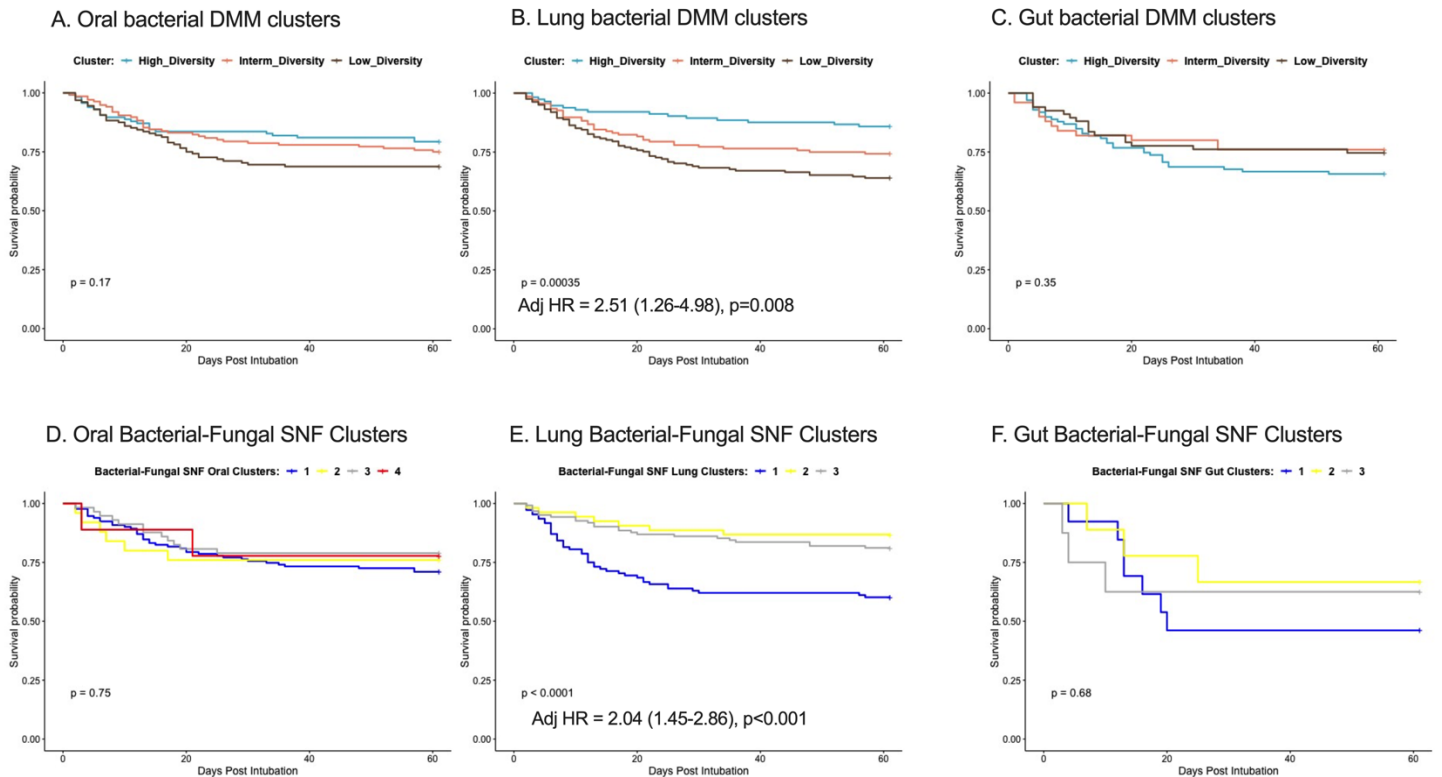
# Bacterial DMM Clusters



739

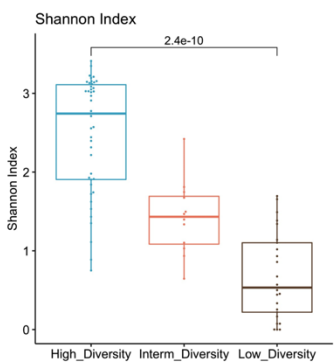
740

741 **Figure 4: Lung bacterial and bacterial-fungal clusters strongly predicted 60-day survival independent**  
742 **of clinical predictors, organ dysfunction severity and host-response subphenotypes.** A-C: Kaplan-Meier  
743 curves for 60-day survival from intubation stratified by oral (A), lung (B) and gut (C) bacterial DMM clusters.  
744 The Low-Diversity lung DMM cluster was independently predictive of worse survival (adjusted Hazard Ratio =  
745 2.51 (1.26-4.98),  $p=0.008$ ), following adjustment for age, sex, history of COPD, immunosuppression, severity  
746 of illness by sequential organ failure assessment (SOFA) scores and host-response subphenotypes. The Lung  
747 bacterial-fungal SNF cluster with high pathogen and *C. albicans* abundance (cluster 1) was independently  
748 predictive of worse survival (D), whereas the oral and gut bacterial-fungal SNF clusters (D, F) did not impact  
749 survival.

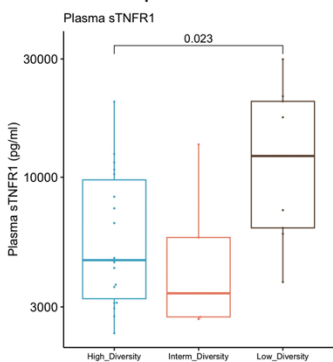


754 **Figure 5: Lung and Gut Microbiota Associations with COVID-19 Severity in Two Independent Cohorts.**  
755 A. Application of the dysbiosis index in lung (ETA) microbiota profiles in the UPMC-COVID cohort classified  
756 subjects in three clusters, with significant differences in Shannon index and bacterial load by 16S qPCR. B.  
757 The low diversity cluster in lung samples from UPMC-COVID subjects was significantly associated with higher  
758 plasma levels of sTNFR1 and Ang-2. C-D. Application of the dysbiosis index models in lung (sputum or ETA)  
759 and gut (stool) samples in the MGH-COVID cohort classified subjects in three clusters, with significant  
760 differences in Shannon index and anaerobe abundance between clusters. E-F: Cluster assignments in the  
761 MGH cohort were strongly associated with clinical severity for lung samples only. Membership in the Low-  
762 Diversity cluster in the lungs was associated with an odds ratio of 8.77 (1.75-61.74) for severe disease (black  
763 belt connecting the Low-Diversity cluster and Severe Disease perimetric zones in the chord diagram). Gut  
764 clusters were not significantly associated with clinical severity of COVID-19 pneumonia.

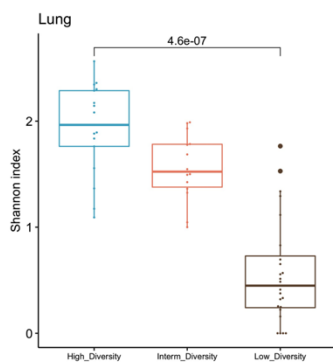
A. UPMC-COVID Lung Clusters



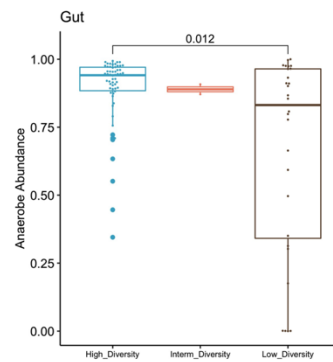
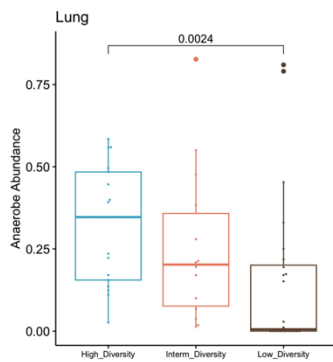
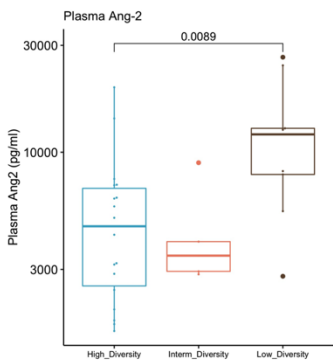
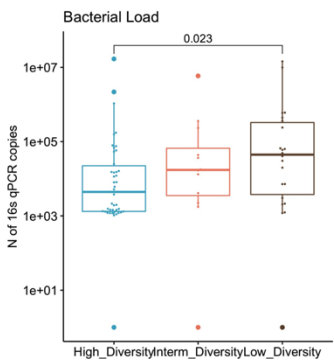
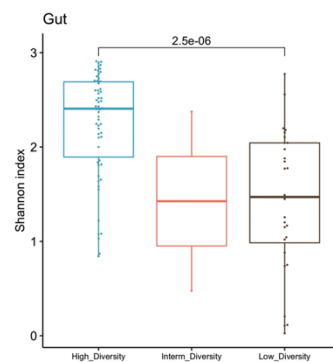
B. Lung Clusters and Plasma Host-Response Biomarkers



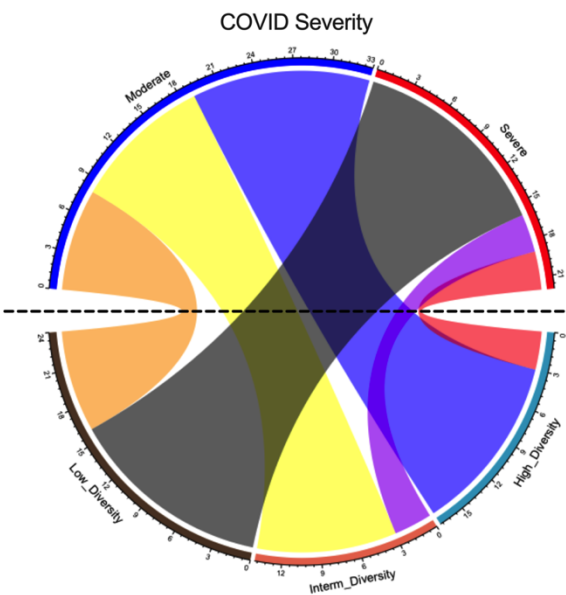
C. MGH-COVID Lung Clusters



D. MGH-COVID Gut Clusters



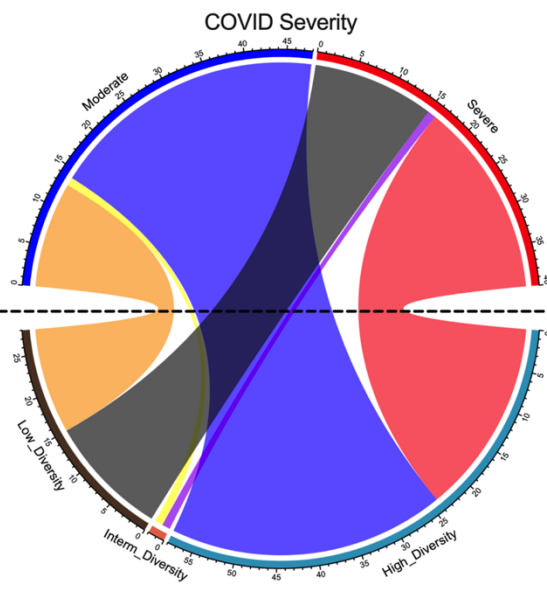
E. MGH-COVID Lung Clusters and Severity



Lung Clusters

OR = 8.77 (1.75-61.74), p=0.003, Low vs. High

F. MGH-COVID Gut Clusters and Severity



Gut Clusters

OR = 1.62 (0.59-4.47), p=0.35, Low vs. High

765  
766  
767  
768  
769

770  
771 REFERENCES  
772  
773  
774

- 775 1. Kitsios, G. D. *et al.* Dysbiosis in the intensive care unit: Microbiome science coming to the bedside. *J.*  
776 *Crit. Care* **38**, 84–91 (2017).
- 777 2. Dickson, R. P. The microbiome and critical illness. *Lancet Respir. Med.* **4**, 59–72 (2016).
- 778 3. Kitsios, G. D. *et al.* Respiratory Tract Dysbiosis Is Associated with Worse Outcomes in Mechanically  
779 Ventilated Patients. *Am. J. Respir. Crit. Care Med.* **202**, 1666–1677 (2020).
- 780 4. Dickson, R. P. *et al.* Lung microbiota predict clinical outcomes in critically ill patients. *Am. J. Respir.*  
781 *Crit. Care Med.* **201**, 555–563 (2020).
- 782 5. Sulaiman, I. *et al.* Microbial signatures in the lower airways of mechanically ventilated COVID-19  
783 patients associated with poor clinical outcome. *Nat. Microbiol.* **6**, 1245–1258 (2021).
- 784 6. Sarma, A., Calfee, C. S. & Ware, L. B. Biomarkers and precision medicine: state of the art. *Crit. Care*  
785 *Clin.* **36**, 155–165 (2020).
- 786 7. Kitsios, G. D. *et al.* Host-Response Subphenotypes Offer Prognostic Enrichment in Patients With or at  
787 Risk for Acute Respiratory Distress Syndrome. *Crit. Care Med.* **47**, 1724–1734 (2019).
- 788 8. Alipanah, N. & Calfee, C. S. Phenotyping in acute respiratory distress syndrome: state of the art and  
789 clinical implications. *Curr. Opin. Crit. Care* **28**, 1–8 (2022).
- 790 9. Heijnen, N. F. L. *et al.* Biological Subphenotypes of Acute Respiratory Distress Syndrome Show  
791 Prognostic Enrichment in Mechanically Ventilated Patients without Acute Respiratory Distress  
792 Syndrome. *Am. J. Respir. Crit. Care Med.* **203**, 1503–1511 (2021).
- 793 10. Kitsios, G. D. *et al.* Distinct profiles of host responses between plasma and lower respiratory tract  
794 during acute respiratory failure. *ERJ Open Research* **9**, (2023).

- 795 11. Fair, K. *et al.* Rectal Swabs from Critically Ill Patients Provide Discordant Representations of the Gut  
796 Microbiome Compared to Stool Samples. *mSphere* **4**, (2019).
- 797 12. Kitsios, G. D. *et al.* The upper and lower respiratory tract microbiome in severe aspiration pneumonia.  
798 *iScience* **26**, 106832 (2023).
- 799 13. Britton, N. *et al.* Respiratory Fungal Communities are Associated with Systemic Inflammation and  
800 Predict Survival in Patients with Acute Respiratory Failure. *medRxiv* (2023)  
801 doi:10.1101/2023.05.11.23289861.
- 802 14. ARDS Definition Task Force *et al.* Acute respiratory distress syndrome: the Berlin Definition. *JAMA* **307**,  
803 2526–2533 (2012).
- 804 15. Nguyen, L. H. *et al.* Metagenomic assessment of gut microbial communities and risk of severe COVID-  
805 19. *Genome Med.* **15**, 49 (2023).
- 806 16. Zhao, J., Murray, S. & Lipuma, J. J. Modeling the impact of antibiotic exposure on human microbiota.  
807 *Sci. Rep.* **4**, 4345 (2014).
- 808 17. Wang, A. A. *et al.* The Narrow-Spectrum Antibiotic Treatment Score: A Novel Quantitative Tool for  
809 Assessing Broad- and Narrow-Spectrum Antibiotic Use in Severe Community-Acquired Pneumonia. in  
810 *B28. HOST AND MICROBIAL CLINICAL STUDIES IN LUNG INFECTIONS AND LUNG DISEASES*  
811 *A2929–A2929* (American Thoracic Society, 2020). doi:10.1164/ajrccm-  
812 conference.2020.201.1\_MeetingAbstracts.A2929.
- 813 18. Holmes, I., Harris, K. & Quince, C. Dirichlet multinomial mixtures: generative models for microbial  
814 metagenomics. *PLoS ONE* **7**, e30126 (2012).
- 815 19. Narayana, J. K., Mac Aogáin, M., Ali, N. A. B. M., Tsaneva-Atanasova, K. & Chotirmall, S. H. Similarity  
816 network fusion for the integration of multi-omics and microbiomes in respiratory disease. *Eur. Respir. J.*  
817 **58**, (2021).



- 818 20. Drohan, C. M. *et al.* Biomarker-Based Classification of Patients With Acute Respiratory Failure Into  
819 Inflammatory Subphenotypes: A Single-Center Exploratory Study. *Crit. Care Explor.* **3**, e0518 (2021).
- 820 21. Kitsios, G. D., Franz, C. & McVerry, v. The Microbiome in Acute Lung Injury and ARDS. in *The*  
821 *Microbiome in Respiratory Disease* (eds. Huang, Y. J. & Garantziotis, S.) (Humana, Cham, 2022).
- 822 22. Lloréns-Rico, V. *et al.* Clinical practices underlie COVID-19 patient respiratory microbiome composition  
823 and its interactions with the host. *Nat. Commun.* **12**, 6243 (2021).
- 824 23. Bernard-Raichon, L. *et al.* Gut microbiome dysbiosis in antibiotic-treated COVID-19 patients is  
825 associated with microbial translocation and bacteremia. *Nat. Commun.* **13**, 5926 (2022).
- 826 24. Chanderraj, R. *et al.* In critically ill patients, anti-anaerobic antibiotics increase risk of adverse clinical  
827 outcomes. *Eur. Respir. J.* (2022) doi:10.1183/13993003.00910-2022.
- 828 25. Pickens, C. O. *et al.* Bacterial Superinfection Pneumonia in Patients Mechanically Ventilated for  
829 COVID-19 Pneumonia. *Am. J. Respir. Crit. Care Med.* **204**, 921–932 (2021).
- 830 26. Kullberg, R. F. J., Schinkel, M. & Wiersinga, W. J. Empiric anti-anaerobic antibiotics are associated with  
831 adverse clinical outcomes in emergency department patients. *Eur. Respir. J.* **61**, (2023).
- 832 27. Kitsios, G. D. & McVerry, B. J. Host-Microbiome Interactions in the Subglottic Space. *Bacteria Ante*  
833 *Portas!* *Am. J. Respir. Crit. Care Med.* **198**, 294–297 (2018).
- 834 28. Dickson, R. P. *et al.* Bacterial topography of the healthy human lower respiratory tract. *MBio* **8**, (2017).
- 835 29. Zhao, T. *et al.* Oral hygiene care for critically ill patients to prevent ventilator-associated pneumonia.  
836 *Cochrane Database Syst. Rev.* **12**, CD008367 (2020).
- 837 30. Hammond, N. E. *et al.* Association Between Selective Decontamination of the Digestive Tract and In-  
838 Hospital Mortality in Intensive Care Unit Patients Receiving Mechanical Ventilation: A Systematic  
839 Review and Meta-analysis. *JAMA* **328**, 1922–1934 (2022).

- 840 31. Klompas, M. Oropharyngeal Decontamination with Antiseptics to Prevent Ventilator-Associated  
841 Pneumonia: Rethinking the Benefits of Chlorhexidine. *Semin. Respir. Crit. Care Med.* **38**, 381–390  
842 (2017).
- 843 32. Buelow, E. *et al.* Comparative gut microbiota and resistome profiling of intensive care patients receiving  
844 selective digestive tract decontamination and healthy subjects. *Microbiome* **5**, 88 (2017).
- 845 33. Horn, K. J., Schopper, M. A., Drigot, Z. G. & Clark, S. E. Airway Prevotella promote TLR2-dependent  
846 neutrophil activation and rapid clearance of *Streptococcus pneumoniae* from the lung. *Nat. Commun.*  
847 **13**, 3321 (2022).
- 848 34. Segal, L. N. *et al.* Enrichment of lung microbiome with supraglottic taxa is associated with increased  
849 pulmonary inflammation. *Microbiome* **1**, 19 (2013).
- 850 35. Wu, B. G. *et al.* Episodic Aspiration with Oral Commensals Induces a MyD88-dependent, Pulmonary T-  
851 Helper Cell Type 17 Response that Mitigates Susceptibility to *Streptococcus pneumoniae*. *Am. J.*  
852 *Respir. Crit. Care Med.* **203**, 1099–1111 (2021).
- 853 36. Dickson, R. P. *et al.* Enrichment of the lung microbiome with gut bacteria in sepsis and the acute  
854 respiratory distress syndrome. *Nat. Microbiol.* **1**, 16113 (2016).
- 855 37. Nath, S., Kitsios, G. D. & Bos, L. D. J. Gut-lung crosstalk during critical illness. *Curr. Opin. Crit. Care*  
856 **29**, 130–137 (2023).
- 857 38. Bain, W. *et al.* Research Bronchoscopy Standards and the Need for Non-Invasive Sampling of the  
858 Failing Lungs. *Ann Am Thorac Soc* (2023).
- 859 39. Shankar-Hari, M., Fan, E. & Ferguson, N. D. Acute respiratory distress syndrome (ARDS) phenotyping.  
860 *Intensive Care Med.* **45**, 516–519 (2019).
- 861 40. Kalil, A. C. *et al.* Management of Adults With Hospital-acquired and Ventilator-associated Pneumonia:  
862 2016 Clinical Practice Guidelines by the Infectious Diseases Society of America and the American  
863 Thoracic Society. *Clin. Infect. Dis.* **63**, e61–e111 (2016).

- 864 41. Morris, A. *et al.* Comparison of the respiratory microbiome in healthy nonsmokers and smokers. *Am. J.*  
865 *Respir. Crit. Care Med.* **187**, 1067–1075 (2013).
- 866 42. Kitsios, G. D. *et al.* Respiratory microbiome profiling for etiologic diagnosis of pneumonia in  
867 mechanically ventilated patients. *Front. Microbiol.* **9**, 1413 (2018).
- 868 43. Charalampous, T. *et al.* Nanopore metagenomics enables rapid clinical diagnosis of bacterial lower  
869 respiratory infection. *Nat. Biotechnol.* **37**, 783–792 (2019).
- 870 44. Yang, L. *et al.* Metagenomic identification of severe pneumonia pathogens in mechanically-ventilated  
871 patients: a feasibility and clinical validity study. *Respir. Res.* **20**, 265 (2019).
- 872 45. Juul, S. *et al.* What's in my pot? Real-time species identification on the MinION. *BioRxiv* (2015)  
873 doi:10.1101/030742.
- 874 46. Huber, W. *et al.* Orchestrating high-throughput genomic analysis with Bioconductor. *Nat. Methods* **12**,  
875 115–121 (2015).
- 876 47. R Foundation for Statistical Computing, R. C. T. *R: A Language and Environment for*  
877 *Statistical Computing.* (CRAN, 2016).
- 878 48. Raghu, V. K. *et al.* Comparison of strategies for scalable causal discovery of latent variable models  
879 from mixed data. *Int. J. Data Sci. Anal.* **6**, 33–45 (2018).